Limnol. Oceanogr., 53(2), 2008, 579–588

Hydrodynamic forces and surface topography: Centimeter-scale spatial variation in wave forces

Michael J. O'Donnell[1] *and Mark W. Denny*
Hopkins Marine Station of Stanford University, Pacific Grove, California 93950

Abstract

We measured the variability in hydrodynamic forces among locations separated by only centimeters along three horizontal transects on a steep rocky shore. Our results extend previous work showing that wave forces have the characteristics of 1/*f*-noise, in which variability in wave forces decreases exponentially with decreasing scales of measurement. Furthermore, our results suggest that protection from hydrodynamic forces is not a certain consequence of a rugose substratum, suggesting that investigators should directly test (rather than assume) small-scale topographic protection from hydrodynamic forces.

The intertidal zone of wave-swept rocky shores is one of the most physically stressful environments on Earth. Perhaps the most apparent physical stress factors—at least to the human observer—are the violent hydrodynamic forces imposed by breaking waves. On exposed shores, water velocities from breaking waves routinely reach 10 m s^{-1}, while storm waves can produce water velocities of greater than 25 m s^{-1} (Denny et al. 2003). The high water velocities in the intertidal zone can impose large hydrodynamic forces on objects they encounter (e.g., Koehl 1984; Denny 1988), and many investigators have examined dislodgement and breakage of organisms subjected to breaking waves (e.g., Shanks and Wright 1986; Trussell et al. 1993; Denny 1995; Gaylord 1999).

Amid these potentially dangerous hydrodynamic forces, wave-swept rocky shores provide habitat for rich and highly diverse communities of species (Ricketts and Calvin 1939; Evans 1947; Stephenson and Stephenson 1972) which have been the subject of intense study, both for their own sake (Dayton 1971; Sousa 1979; Lohse 1993) and as a model system for community ecology in general (Wethey 1985; Gaines and Bertness 1993; Underwood 2000). Understanding the degree to which physical factors such as wave exposure (Trussell 1997*a*; Gaylord 1999; Rilov et al. 2004) or temperature (Helmuth 1998; Somero 2002) determine where organisms live has been a common theme in many intertidal studies. For example, distributions of intertidal organisms are often patchy (Paine and Levin 1981); if aspects of the physical environment determine the limits of habitable space for certain species, then understanding the patchiness of environmental conditions can potentially help to explain the patchy distributions of organisms. On the rugose rock surfaces of wave-swept shores, interactions between substratum topography and wave-induced flow may create such a spatially variable environment.

Topography

Numerous investigators have explored how distributions of organisms are influenced by the topography of intertidal substrata. A concept often invoked is that of "microhabitats," areas within a larger habitat with different environmental conditions from the average of their surroundings. What, precisely, comprises a microhabitat depends on the system and question of interest. For instance, a protected bay could constitute a microhabitat within an otherwise exposed coastline, while a shaded region beneath a rock may be a microhabitat of an otherwise sunny shore (*see* McGuinness and Underwood 1986 for further discussion). Ecologists hoping to understand the distributions of organisms often divide experiments into individual field sites where they collect samples along transects or within quadrats. A sampling unit is generally chosen so that environmental parameters that may influence organismal distributions are as constant as possible within it. Regions of variability within quadrats or transects could constitute microhabitats and might increase the measured variability of organismal distributions. Hydrodynamic stresses from breaking waves and temperature stresses due to aerial exposure at low tide are important environmental parameters in the wave-swept intertidal region. Both of these environmental parameters can be affected by the topography of the shoreline, with physical structures modifying the environment in the region immediately surrounding them (e.g., temperature; Marchetti and Geller 1987; Jones and Boulding 1999; Helmuth and Hofmann 2001).

A number of investigators have also explored interactions between surface topography and wave exposure to help explain organismal distribution patterns. For instance,

[1] Present address: Marine Science Institute, University of California–Santa Barbara, Santa Barbara, California 93106-9150.

Acknowledgments

We thank Luke Hunt, Luke Miller, Chris Harley, Vanessa Hume, Patrick Martone, Joanna Nelson, Lisa Walling, Kim Heiman, Katie Mach, and Suzanne Cowden who assisted with field placement, data collection, dynamometer calibration and more. John Lee assisted with the dynamometer design and construction. Ed Thornton lent GPS mapping equipment. Two anonymous reviewers made helpful improvements to the manuscript.

This project was funded in part by NSF grant OCE-9985946 to MWD. This is contribution No. 269 of the Partnership for Interdisciplinary Studies of Coastal Oceans (PISCO), a long-term consortium funded primarily by the Gordon and Betty Moore Foundation and David and Lucile Packard Foundation.

increasing the relief of rock surfaces by drilling holes led to large increases in populations of snails (Emson and Faller-Fritsch 1976; Addy and Johnson 2001). Tracking snails revealed preferential movement from topographically simple locations into those with more structural complexity (McGuinness and Underwood 1986; Underwood and Chapman 1989). In a settlement experiment, Underwood (2004) showed that the response of juvenile gastropods to surface topography is highly species-specific. In another study on wave exposed shores, predatory snails had the largest effect on prey that lived within easy reach of protected crevices, and investigators proposed that this could be explained by crevices offering less dangerous hydrodynamic conditions (Menge 1976; Menge 1978). Trussell (1997*b*) noticed a shift in the sizes of snails on a shore following a storm event with large waves, and postulated that the shells of surviving snails were better suited to take advantage of the refuge offered by crevices. There is ample evidence that the distributions of organisms are influenced by rugose surfaces, but the mechanisms driving these effects, especially with regards to hydrodynamic forces, are only partially understood.

This study investigated whether microhabitats, hydrodynamically protected from the harsh environment, might permit organisms to live where they otherwise could not. For this to be the case, wave forces must vary over short enough distances that mobile organisms can expect to find protection available as they move around on wave-exposed rocks.

Another area of intense interest to intertidal ecology is an understanding of the spatial scales of variation in biological and abiotic parameters. Underwood and Chapman (1996) measured the variability of organismal abundance in 0.25-m^2 quadrats along kilometers of shoreline in southwest Australia and found that there was more variation between consecutive quadrats than between quadrats separated by tens or even thousands of meters. They postulated that the environment varied most between locations <1 m apart and that mobile organisms responded to the environment, thereby creating a pattern of small-scale biological variation. This postulate was commensurate with other studies on the effects of topography on wave swept shores in which it was assumed that small-scale substratum topography reduces the severity of wave shock (e.g., Addy and Johnson 2001; Menge 1978; Trussell 1997*a*), or that organisms in sites with less topographical complexity experienced greater wave shock (e.g., Underwood and McFadyen 1983). In contrast, Denny et al. (2004) made regularly spaced measurements along 334 m of shoreline in central California and found that variability in several environmental and biological parameters, including wave exposure, decreased exponentially with decreasing spatial scale of measurement, a pattern known as $1/f$-noise. However, the measurements of Denny et al. were spaced 0.5 m apart and therefore could not discern variability at spatial scales below 1 m. The trend of decreasing variability with decreasing scale could be reversed at a scale small enough to include measurements within the type of crevices and pits utilized for shelter by intertidal organisms.

Previous studies have not directly measured the wave forces imposed on objects smaller than several centimeters, nor have they measured the variation in wave forces over the small spatial extents through which intertidal organisms commonly move. In response to this problem, and to better resolve the general pattern of scale-dependent variation in wave exposure, we quantified hydrodynamic forces imposed on objects $\sim$1 cm in diameter and took measurements at higher spatial resolutions (i.e., with measurement points spaced sufficiently close together) to observe differences caused by topographic features such as crevices. We used these measurements to address two questions: (1) Does the variability in hydrodynamic forces increase or decrease at small spatial scales? and (2) Can crevices always be assumed to provide shelter from wave-induced forces?

Methods

Dynamometers—To measure hydrodynamic forces experienced by objects in the intertidal zone, we adapted the dynamometer design described by Denny and Wethey (2001) and used by Helmuth and Denny (2003). They provide an index of the maximum wave exposure of a site, useful for comparisons between locations, and have a long history in intertidal studies (Jones and Demetropoulos 1968; Bell and Denny 1994). Briefly, these meters recorded the maximum hydrodynamic force imposed on a roughened sphere, which was connected to a spring via a string equipped with a rubber slider. The spring, string, and slider were housed in a piece of rigid tubing with a threaded neck. The device was inserted into a hole drilled in the substratum and secured to a threaded collar such that only the ball and the threaded neck sat above the rock. Hydrodynamic forces moved the ball, extending the spring and causing the slider to move down the string. Upon recovery, the slider remained in the position of maximum displacement, providing a record of the maximum hydrodynamic force exerted on the ball during the deployment. For this experiment, we constructed diminutive dynamometers with drag spheres either 0.47 cm or 0.95 cm in diameter. (The small size was used in areas of very high force.) The springs on these devices had a maximum extension of $\sim$1 cm, hence these dynamometers measured the maximum force experienced somewhere within a circle of $\sim$2 cm radius, an order of magnitude smaller than previous investigations. Each dynamometer was calibrated, either by hanging weights from the measurement ball and calculating the force due to gravity, or by pulling the dynamometer against a calibrated load cell that measured forces directly. The displacement of the slider was measured for each force. On average, dynamometers could record a minimum force of 1.7 N (set by the initial tension of the spring) and a maximum of $\sim$9 N.

Site placement—We deployed dynamometers in horizontal transects at three sites in the intertidal zone at the Hopkins Marine Station in Pacific Grove, California. Each transect was centered on a measurement location from Denny et al. (2004) at a constant tidal height of $\sim$1.7 m above Mean Lower Low Water (MLLW, NTDE 1983–2001). Holes were drilled every 5 cm to the left and right of the earlier measurement location. Thus, this study embed-

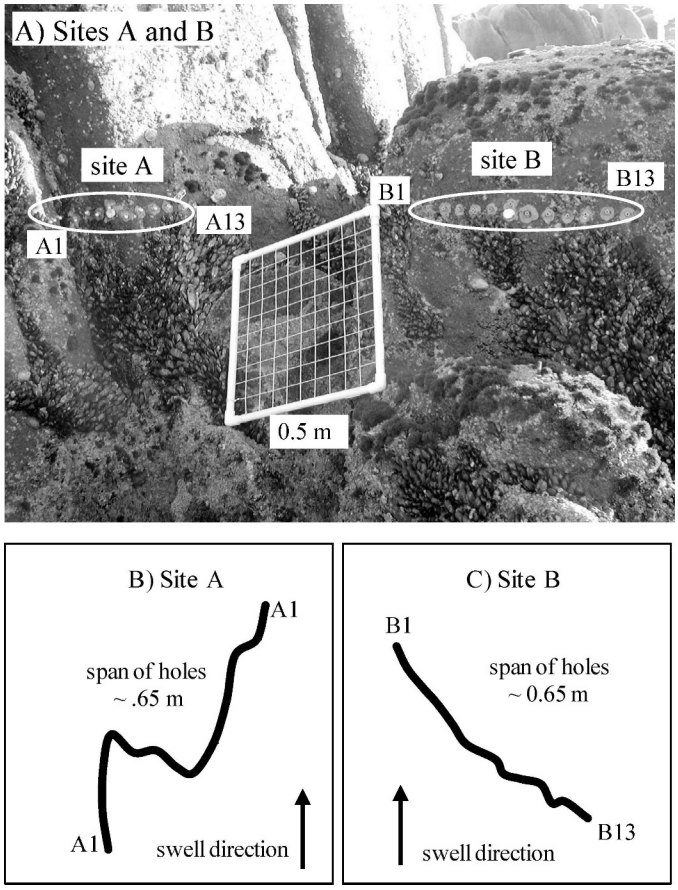

Fig. 1. (A) Photograph of sites A and B on the rock. Measurement holes are small patches between labels A1–A13 and B1–B13. The small white dots (outlined with ovals) are the drag spheres of dynamometers. The quadrat in the center of the picture is 0.5 m per side for scale. (B) Sketch of overhead view of the contour of the rock surface at site A. (C) Sketch of overhead view of the contour of the rock surface at site B.

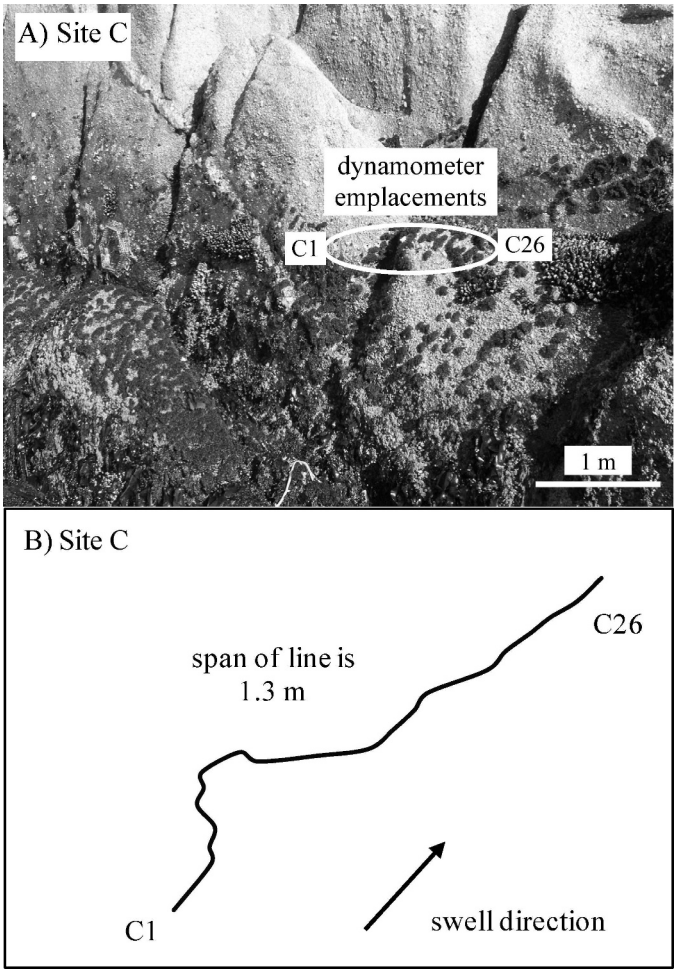

Fig. 2. (A) Photograph of site C on the rock. Measurement holes are outlined with oval between labels C1 and C26. (B) Sketch of overhead view of the contour of the rock surface.

ded a finer scale of measurement within the previous results of Denny et al. At the central location, a hole was located ~2 cm above the transect to avoid the existing mounting hole. These transects were designated as A, B, and C, with each hole at a site numbered from left to right when facing the rock (*see photographs in Figs. 1, 2*).

One goal of this project was to determine the maximum, rather than the average, level of variation in wave force between closely spaced sites. Accordingly, we selected sites from Denny et al. (2004) that had a high degree of variation in wave forces between locations only 0.5 m apart (sites A and B) or 4 m apart near site C. Fig. 3 shows a selection of data from Denny et al. highlighting the level of variation in wave force surrounding sites A and B.

Another goal of the study was to explore the effects of rock topography on the maximum forces that objects experience beneath breaking waves. To this end, we chose sites that shared some common aspects of their topography: All were on vertical surfaces that faced the prevailing swell direction (within ~45°). Site A had a deep crevice, ~25 cm wide and ~15 cm deep, running vertically through the site, encompassing holes A3, A4, and A5. Site B had a small crevice, ~5 cm wide and ~2 cm deep, encompassing hole B10. Site C had a crevice running vertically through it, ~20 cm wide and ~10 cm deep at holes C6–C8 (*see sketches in Figs. 1, 2*).

Significant wave height—We measured significant wave height offshore (H_S) using a Seabird SBE26 Wave Height Meter (SeaBird Electronics). Significant wave height, a common index of sea state, is the average height of the highest one third of waves (Kinsman 1965). The meter was mounted in ~10 m of water in a kelp bed ~125 m from the intertidal sites. The meter measured surface elevation at 4 Hz for 8.53 min every 6 h in order to compute the significant wave height.

Dynamometer force measurements—We attempted to leave dynamometers deployed in the field for only a single day between deployment and readout (78% of the measurements were 1-d deployments, 11% were 2-d deployments, the maximum was 9 d). On each workable low tide (as determined by tidal height and wave exposure), we recovered previously installed meters and measured the

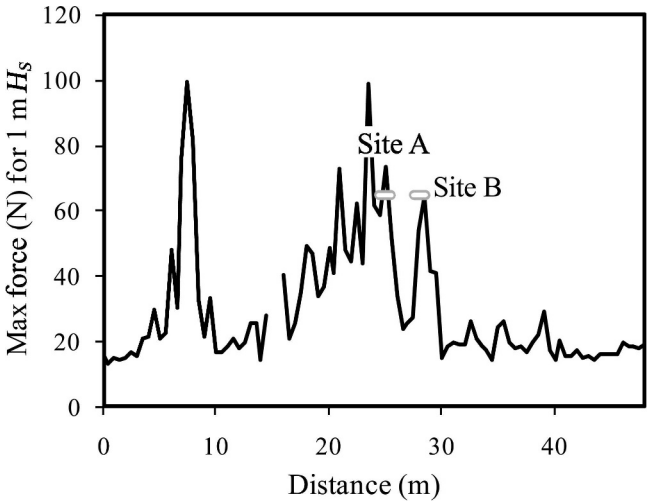

Fig. 3. Maximum force data from Denny et al. (2004, Electronic Appendix E6). Each point is spaced 0.5 m apart, at a constant tidal height. Forces are predicted for each location for significant wave height of 1 m. Sites for the current study were chosen from this graph by selecting locations with a high degree of variation in wave force between sites 0.5 m apart. Site C is not shown in this graph, but had a similar degree of variation.

maximum displacement of their rubber sliders using electronic digital calipers. Because of the difficulty of measuring these small displacements, we took three separate measurements of each displacement and used an average for later analysis. Each displacement was converted to a force. In practice, we were able to measure displacements $\geq$0.5 mm; these extremely low measurements served primarily to demonstrate that the meter had experienced a force greater than the initial tension of the spring. Meters with displacements $<$0.5 mm, were recorded as "none detected" and excluded from further analysis.

At certain measurement locations (especially A3, A4, and A5), forces on 0.95-cm-diameter balls reached the maximum limit on the dynamometer on a large number of days. For these sites, we used dynamometers with drag spheres 0.47 cm in diameter; smaller drag spheres reduced the imposed force to within the measurement range of the device.

Dynamometer analysis—To compare measurements from meters that had different size drag spheres, we normalized them to an equivalent drag on a 1-cm drag sphere. The drag force on a sphere due to steady flow can be described by the equation:

$$\mathrm{F} = \tfrac{1}{2}\rho U^2 A_F C_D \tag{1}$$

where U is water velocity, ρ is the density of the fluid, A_F is the frontal area of the object presented perpendicular to the flow, and C_D is an empirically-derived dimensionless coefficient of drag. Although Eq. 1 only describes steady flow, previous empirical work (Gaylord 2000) has demonstrated that for objects approximately the size of these spheres, the elementary drag equation is often the best predictor of maximum forces. The drag coefficient varies with the Reynolds number (Re) of the flow, which is also a function of the velocity, U (Bearman and Harvey 1976). Re expresses the relationship between inertial and viscous forces in a fluid.

$$\mathrm{Re} = UL/v \tag{2}$$

Here, L is some characteristic length scale of the flow situation (in this case, the diameter of the drag sphere) and v is the kinematic viscosity of the fluid.

Denny et al. (unpubl. data) measured a relationship between drag coefficient and Re for roughened spheres. This relationship was measured over the Re range of 10^5–10^6 using roughened spheres (such as those used here as drag spheres) in turbulent, air-entrained flows (similar to those found in surf). These calculations resulted in a relationship very similar to the standard relationships often shown in fluid dynamics textbooks.

$$\begin{aligned}\log10(C_D) = {} & 0.6947[\log_{10}(\mathrm{Re})]^3 - 11.218[\log_{10}(\mathrm{Re})]^2 \\ & + 59.91\log_{10}(\mathrm{Re}) - 106.31\end{aligned} \tag{3}$$

From Eq. 3, we used an iterative process to estimate the drag coefficient for each flow measurement. An average C_D of 0.45 was used to estimate a flow velocity that caused a given force. This initial velocity was used to estimate the Re of the flow situation, which was used to calculate a better estimate of the C_D according to Eq. 3. This process rapidly converged on a C_D, which was then used to estimate flow velocity. This velocity, in turn, was used to predict the force that would have been imposed on a sphere 1 cm in diameter.

For each measurement hole, we plotted the force from each dynamometer against the highest significant wave height (H_S) measured by the wave meter during the deployment period. Following the method of Helmuth and Denny (2003), we fit these points either with a linear regression or a function that assumes that with increasing wave height, force asymptotically approaches a maximum value.

$$\mathrm{Force}_{\mathrm{predicted}} = F_a\,(1 - \exp(-H_S/I_h)) \tag{4}$$

Here, F_a is the asymptotic force and I_h is the wave height at which maximum force is within 37% ($=1/e$) of F_a. This model assumes that an upper limit exists, and we fit the data to the equation in order to estimate that limit. Using Prism 4 (GraphPad Software), we fit both linear and asymptotic functions and selected as the best fit the equation that accounted for the largest fraction of overall variance. That is, we chose the fit with the largest r^2 value.

Spatial frequencies of measurement—Because our measurement points were evenly spaced, 5 cm apart, we were able to explore the variation in wave forces at higher spatial frequencies than those presented by Denny et al. (2004). The total variance of maximum force measured along each transect could be divided among wave numbers, the spatial equivalent of frequency for a signal that varies in space rather than time. The wave number has units of cycles L^{-1}, where L is the distance over which the pattern repeats itself.

Spectral density, analogous to probability density, is the proportion of the total variance of the signal associated with a given range of wave numbers. If most of the variability in maximum wave forces is explained by differences between measurements taken only short distances apart (which equate to high wave numbers), spectral density at high wave numbers is greater than at lower wave numbers. If, however, there is less variability between closely spaced locations and most of the total variability is due to measurements taken far apart, spectral density is higher at low wave numbers.

The dynamometers used by Denny et al. (2004) had larger drag spheres than those here: 4.1 cm in diameter versus a scaled diameter of 1 cm. As noted, this change in size also led to a change in the drag coefficient of the spheres. To combine the data from this study with that from Denny et al. (2004), we used the velocity term from Eq. 1 to scale the measurements from this study up to the forces expected had the ball been 4.1 cm in diameter. Our transects of data were divided into three segments with 50% overlap, and the spectra were computed for each segment, then averaged according to the method of Denny et al. (2004; *see Appendix A for details of method*).

Results

Three representative regressions of force to significant wave height are shown in Fig. 4, spanning the range of r^2 values obtained. In general, H_S is a poor predictor of force experienced by these dynamometers. At 22 of the microsites, the asymptotic function provided a better fit than a linear, unbounded function. At the remaining 25 sites, a linear function provided a better fit, or the software could not converge on a solution for the asymptotic function. To summarize the different fits, we used the distinctions from Helmuth and Denny (2003) who described fits as either significant and substantial ($p \leq 0.05$, $r^2 \geq 0.25$), significant but not substantial ($p \leq 0.05$, $r^2 \leq 0.25$), or not significant ($p \geq 0.05$). For a large fraction of our sites (53%), the relationship between force and H_S was not statistically significant. An additional 26% had a relationship that was statistically significant but not substantial. In only 28% of these measurement locations did H_S explain a substantial portion of the variation in force. These results differ from those of Helmuth and Denny (2003), who found a significant and substantial relationship between force and H_S at 66% of their sites.

To make comparisons among sites, we used the regressions between maximum force and significant wave height to calculate the maximum force that would be expected for certain values of H_S. Data for 50-cm and 150-cm H_S are presented in Figs. 5 and 6. These values approximately correspond to the 20th and 92nd percentiles of wave heights recorded in a typical year, spanning a large fraction of the range of conditions experienced at this stretch of coastline.

These graphs highlight the narrow range of maximum forces experienced among sites. At most sites, a 1-cm ball might be expected to experience a maximum force of ~4 N during the course of a day when the significant wave height

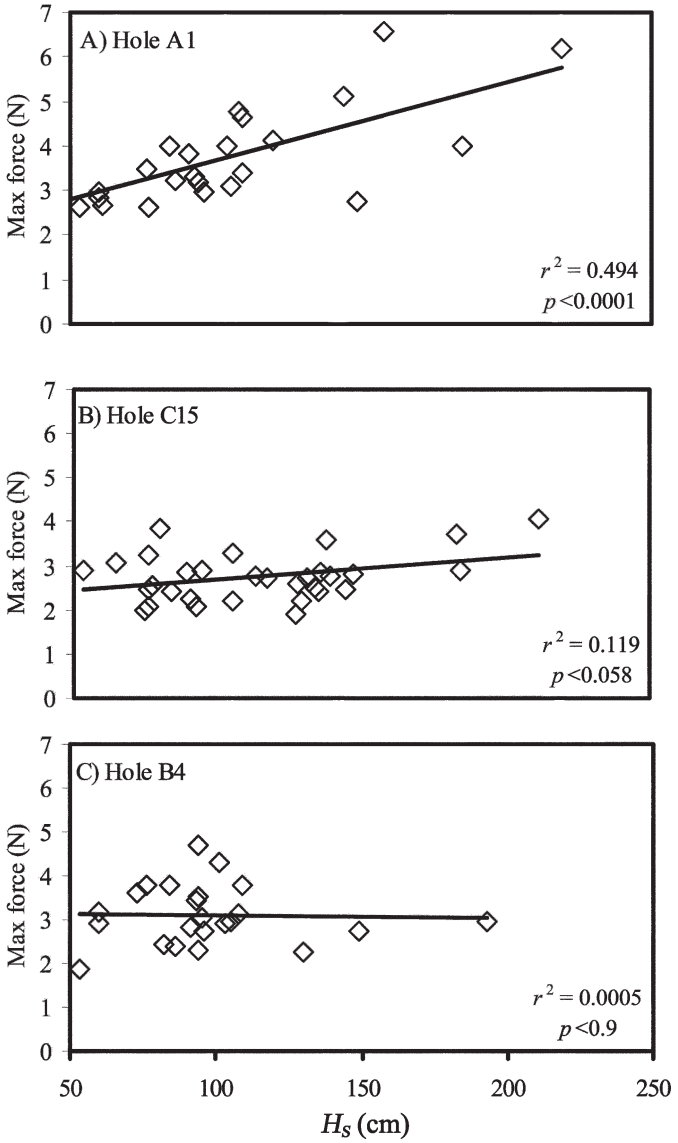

Fig. 4. Representative holes showing different relationships between H_S and the force experienced by dynamometer ball 1 cm in diameter. Hole A1 has the highest r^2 of any of the locations, Hole C15 has approximately the median r^2 of the measurement locations, and hole B4 has the lowest r^2 of any location. The slope of hole A1 was both significantly different from zero and explained a substantial portion of the variance. At hole C15, the slope was significantly different from zero, but the r^2 was not substantial. For hole B4, the slope was not significantly different from zero.

is 150 cm. These results are consistent with the poor relationship noted between force and significant wave height. Our sampling locations were chosen to test the spatial frequency of variability, rather than the specific effect of crevices on wave forces. However, the data in Figs. 5 and 6 show that the locations within crevices (marked with a "C") do not experience reduced wave forces relative to nearby sites. The only observable difference was that the forces within the crevice at holes A2–A5 tended to be higher than at nearby sampling locations. As a simple test of whether forces were different within the crevices

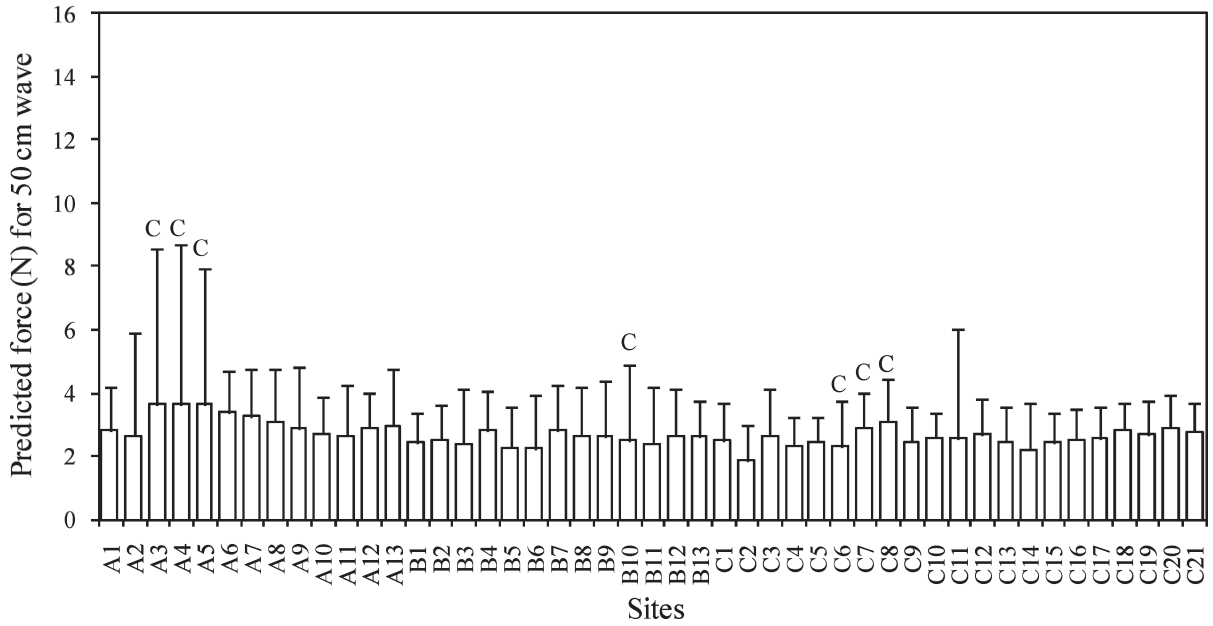

Fig. 5. Forces predicted on a ball 1 cm in diameter for 50-cm offshore significant wave heights, H_S. Error bars are 95% confidence intervals. A "C" above a bar indicates that the site is within a crevice.

versus outside the crevices, we chose paired measurements for a crevice location and a location 10-cm away where meters had been deployed on the same day. (This distance was chosen to avoid comparisons with meters ambiguously close to the edge of the crevice.) We compared the forces experienced by each pair of locations using a paired *t*-test and examined how the different sites inside and outside of crevices responded to identical wave conditions. The results of this analysis are presented in Table 2. For the three crevices explored here, there was no evidence that crevices reduce wave forces. Where any differences were detected between holes within crevices and those nearby, the forces were higher within crevices.

Spatial frequencies of measurement—Spectral density of wave force was plotted against wave number in Fig. 7 using data from this study and from Denny et al. (2004). Data from the present study continued the 1/*f*-noise trend seen by Denny et al., with variation decreasing at finer spatial scales of measurement. Data from this study represent the highest spatial frequencies with which wave forces have been measured along a shoreline.

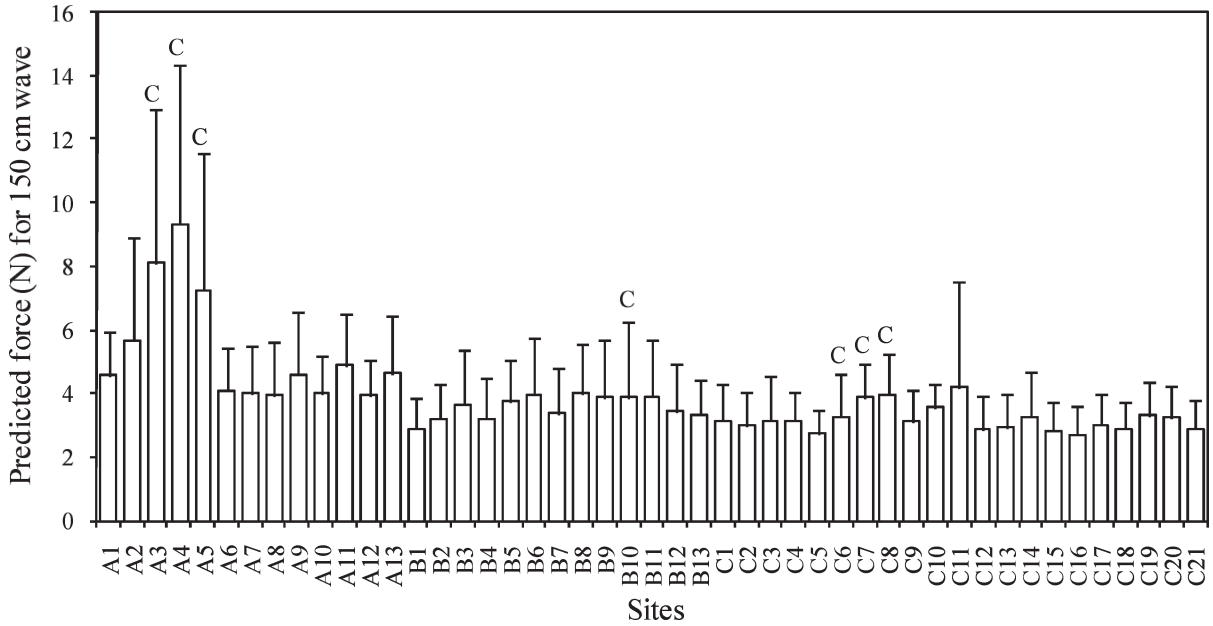

Fig. 6. Forces predicted on a ball 1 cm in diameter for a 150-cm offshore significant wave heights, H_S. Error bars are 95% confidence intervals. A "C" above a bar indicates that the site is within a crevice.

Table 1. Regression coefficients and model choice for each measurement hole. F_a and I_h are reported only for holes where the asymptotic fit resulted in a higher r^2. p-values were calculated for the linear fit for each hole; where the linear slope was not significantly different from zero, we assumed that no significant relationship between force and offshore wave height existed.

	Preferred model	n	Best r^2	Linear slope (N/cm H_S)	Linear intercept (N)	p value	F_a (N)	I_h (cm)
A01	linear	25	0.494	0.017	1.936	<0.0001		
A02	linear	27	0.416	0.030	1.131	0.0003		
A03	asymptotic	28	0.332	0.037	2.320	0.0014	12.840	150
A04	linear	25	0.457	0.057	0.803	0.0002		
A05	linear	26	0.243	0.036	1.840	0.0105		
A06	linear	28	0.107	0.007	3.003	0.0895		
A07	linear	26	0.159	0.007	2.869	0.0439		
A08	linear	26	0.081	0.008	2.695	0.1596		
A09	asymptotic	27	0.242	0.012	2.689	0.0166	4.995	59
A10	asymptotic	28	0.306	0.012	2.321	0.0025	4.201	48
A11	linear	26	0.447	0.022	1.554	0.0002		
A12	asymptotic	27	0.240	0.007	2.882	0.0183	4.032	39
A13	linear	28	0.313	0.016	2.159	0.0020		
B01	asymptotic	28	0.078	0.004	2.326	0.1550	2.901	28
B02	asymptotic	29	0.141	0.004	2.590	0.2217	3.264	34
B03	asymptotic	33	0.150	0.011	2.121	0.0383	3.866	52
B04	asymptotic	23	0.037	−0.001	3.164	0.9157	3.211	24
B05	asymptotic	32	0.305	0.013	1.842	0.0016	4.100	62
B06	asymptotic	35	0.241	0.016	1.683	0.0042	4.614	76
B07	asymptotic	35	0.068	0.002	2.999	0.6676	3.366	27
B08	linear	31	0.262	0.014	1.956	0.0033		
B09	linear	36	0.157	0.013	1.967	0.0166		
B10	asymptotic	37	0.105	0.011	2.289	0.0844	4.140	54
B11	linear	31	0.279	0.015	1.650	0.0022		
B12	asymptotic	30	0.076	0.006	2.568	0.1756	3.477	35
B13	asymptotic	30	0.100	0.006	2.535	0.0935	3.383	34
C01	linear	27	0.167	0.007	2.147	0.0341		
C02	asymptotic	31	0.233	0.007	1.928	0.0168	3.229	58
C03	asymptotic	29	0.024	0.002	2.799	0.5186	3.172	28
C04	linear	30	0.329	0.008	1.930	0.0009		
C05	linear	29	0.103	0.003	2.310	0.0895		
C06	linear	33	0.272	0.010	1.819	0.0019		
C07	asymptotic	35	0.115	0.004	3.235	0.0921	3.958	38
C08	asymptotic	35	0.072	0.004	3.330	0.1765	4.009	34
C09	asymptotic	31	0.065	0.003	2.659	0.2938	3.151	33
C10	asymptotic	36	0.219	0.005	2.802	0.0058	3.665	41
C11	linear	38	0.139	0.016	1.753	0.0212		
C12	asymptotic	32	0.005	0.000	2.884	0.9003	2.857	17
C13	linear	32	0.120	0.005	2.224	0.0526		
C14	linear	29	0.314	0.011	1.673	0.0016		
C15	linear	31	0.118	0.004	2.228	0.0580		
C16	linear	34	0.026	0.002	2.424	0.3638		
C17	asymptotic	32	0.037	0.002	2.678	0.3005	3.036	27
C18	linear	27	0.003	0.001	2.819	0.7699		
C19	linear	28	0.184	0.006	2.357	0.0228		
C20	linear	30	0.062	0.003	2.727	0.1861		
C21	linear	30	0.016	0.001	2.694	0.5036		

Discussion

These results provide insight into aspects of the hydrodynamic environment of wave-swept shores. Because we measured maximum wave forces on objects 1 cm in diameter spaced only 5 cm apart, these results illuminated the conditions experienced by the many intertidal organisms with body sizes ~1 cm. In particular, these results helped to discern how forces varied through space and in relation to surface topography.

At this scale, significant wave height was a poorer predictor of wave force on 1-cm-diameter balls than it was for forces measured on 4.1-cm-diameter balls by Helmuth and Denny (2003). Only 49% of our holes had a slope of force versus H_S that was significantly different from zero, compared with 83% for the measurements of Helmuth and Denny. This may have been due to differences in our measuring devices. Due to their size, the small dynamometers used in this study had a much faster response time. Simply moving the ball from one side of the meter to the

Table 2. Paired comparisons between simultaneous maximum wave forces at measurement points within crevices and measurement points 10 cm away, outside of crevice. Looking at a point two measurement locations away avoided holes close to the edge of the crevice. At B10, with only a single meter in the crevice, B08 was randomly selected for comparison. In only one case (A01 vs. A03) was the difference between the two significantly different than zero. At A01, A05 and C08, the in-crevice force was significantly larger than the out-of-crevice force. In no case was the out-of-crevice force significantly larger than the force at the measurement point within the crevice.

Paired comparison	df	Prob>|*t*|	Prob>*t*	Prob<t
A01 (crevice) vs. A03 (non-crevice)	18	0.002	0.001	0.999
A05 (crevice) vs. A07 (non-crevice)	16	0.022	0.011	0.989
B10 (crevice) vs. B08 (non-crevice)	23	0.870	0.565	0.435
C06 (crevice) vs. C04 (non-crevice)	25	0.673	0.664	0.336
C08 (crevice) vs. C10 (non-crevice)	25	0.068	0.034	0.966

other and stretching the spring took several milliseconds for the larger dynamometers of Helmuth and Denny, but only fractions of a millisecond for the meters used in this study. It is therefore possible that our measurements responded to rapidly changing, stochastic events that were less dependent on the size of waves.

Across the 47 locations where maximum wave forces were quantified, data showed few significant differences among holes, and those sites that had forces significantly different from others (in this case, sites within crevices) experienced higher forces than their surroundings.

The data presented here support the conclusion of Denny et al. (2004) that, on this shore, variation in wave forces decreases with decreased scale of observation. Consider an organism crawling along a rock surface: Over tens of centimeters, it is likely to find fairly similar

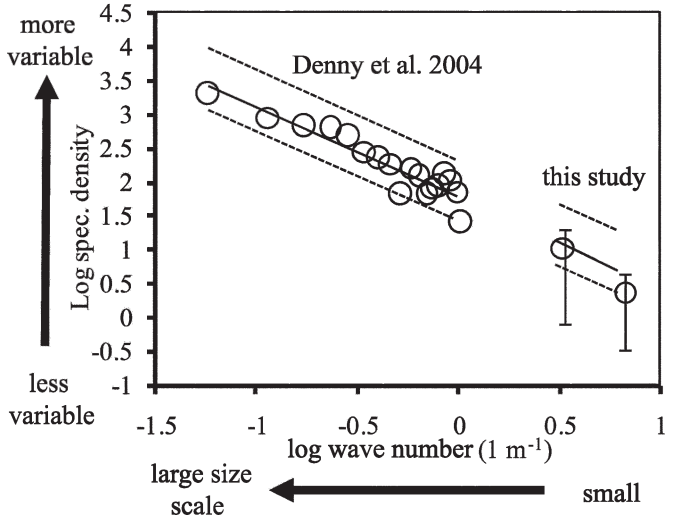

Fig. 7. Spatial spectrum of wave height along transect from Denny et al. (2004) and from this study. Dashed lines are regressions of 95% confidence intervals for individual points. The regression and confidence intervals are extrapolated from Denny et al. (2004) to illustrate that these current data fall within their predictions. The data points from this study are averages and SE bars of frequencies computed from three transects. Transect C was split into two transects of 13 points each in order to examine the same wave numbers as the other two transects. The X-axis is the $\log_{10}$ of the wave number, where wave number is the spatial frequency being considered. The Y-axis is the $\log_{10}$ of the spectral density (in N^2 m).

environmental conditions (the same result predicted by Denny et al.). Even if it does find differences in wave forces by crawling such short distances, those differences pale in comparison to the differences in wave forces that might be experienced between this organism and one tens or hundreds of meters away. In contrast, Underwood and Chapman (1996) found that there was more variation in abundances between measurement locations <1 m apart than between locations ten and even thousands of meters apart. This discrepancy may be a function of topographical differences between the two study systems.

Surface topography—Over the short regions of shoreline explored here, we did not document any protection from maximum wave forces due to crevices. These results indicate that closely spaced refuges from high water velocities may not be as ubiquitous on rocky intertidal shores as previously believed. Additionally, the enhancement of water velocity that we measured in a crevice indicates that crannies in rock should not be automatically considered to be refuges from wave force.

Careful observation of waves striking Site A suggests that the enhanced forces measured in this crevice (A3–A5) are due to complex interactions between breaking waves and the topography of rocks a considerable distance upstream from the crevice in question. By the time waves are fully broken on the shore, the direction of the prevailing swell may not be the most relevant direction to describe waves. Once broken on rocks, turbulent bores are reflected and refracted by many different features on the shore and often approach from directions other than that of the original swell. Denny et al. (2003) found that when waves traveling over a horizontal surface contact a vertical wall, the resultant splash up the wall may have velocity considerably higher than the original jet of water (1.3–1.6 times faster). However, because all of our sites were on vertical surfaces, all would be subjected to these amplified velocities, and this phenomenon cannot wholly explain the higher wave forces within this crevice.

Reducing flow velocity is not the only mechanism by which topography may provide protection for intertidal organisms. Crevices, pits, holes, and other topographic features may also act to improve the ability of organisms to remain attached to their substratum, even in the face of enhanced water velocities. Consider the case of a hypothetical snail, 1 cm in diameter, being struck by a wave. The snail adheres to the rock with the mucus under its foot.

Moving water imposes drag and lift forces on the shell (in the direction of and perpendicular to the flow direction, respectively). These are transferred to the foot through the visceral mass, along with a moment from the rotation of the shell. (A moment is a measure of the tendency of a force to cause a body to rotate around a fixed axis.) If the sum of these effects exceeds the ability of the foot to attach to the substratum, the snail will be dislodged. If, however, the snail were on a surface covered with snail-size bumps or near a crevice wall, it might use these to its advantage. By pressing the downstream side of its shell against rigid structures, the force in the direction of flow would be transferred from the shell to the rock surface without imposing stress on the foot. Similarly, moments, which would peel the foot off the substratum, would be greatly reduced. Given the variability of direction of force, it would be helpful to a snail to have protrusions of the rock on several sides of its shell, like those which might occur inside a crevice only slightly larger than its shell. In this manner, snails like those observed by Raffaelli and Hughes (1978), which prefer crevices only slightly larger than their shells, may be experiencing protection from dislodgement without any reduction of the water flow (and, therefore, the hydrodynamic force) imposed on the snail.

Such mechanisms deserve additional consideration in light of this study. The hydrodynamic forces presented here do not provide evidence for force reductions due to topographic features at our sites. Relative to the average expected forces at the measurement sites, no group of holes experienced significantly lower forces. This is not to claim that crevices categorically enhance hydrodynamic forces, far from it. Rather, it merely demonstrates that force amplification in crevices is possible, and that caution should be exercised when drawing conclusions about hydrodynamic forces and surface topography. If a particular interpretation of a biological observation suggests that forces are lower in a particular crevice (e.g., snails congregate in the crevice when waves are high), investigators would be wise to measure forces directly.

In the future, measurement tools should be developed that would permit investigation of the wave forces within crevices smaller than those we considered. Although the dynamometers used in this study provide some of the finest spatial resolution of forces ever recorded in the surf zone, the measurement spheres are still large relative to many of the organisms that inhabit this region, and the crevices in which they could be installed were, unfortunately, larger than those where other investigators have documented increases in organismal abundance (e.g., Emson and Faller-Fritsch 1976; Raffaelli and Hughes 1978). Measurements at an even finer spatial resolution might reveal hitherto unnoticed levels of variation that would be of great biological interest.

References

Addy, T. C., and L. E. Johnson. 2001. Littorine foraging behavior and population structure on a wave-exposed shore: Nonlinear responses across a physical gradient. J. Shellfish Res. **20:** 385–391.

Bearman, P. W., and J. K. Harvey. 1976. Golf ball aerodynamics. Aeronaut. Quart. **27:** 112–122.

Bell, E. C., and M. W. Denny. 1994. Quantifying "wave exposure": A simple device for recording maximum velocity and results of its use at several field sites. J. Exp. Mar. Biol. Ecol. **181:** 9–29.

Dayton, P. K. 1971. Competition, disturbance, and community organization: The provision and subsequent utilization of space in a rocky intertidal community. Ecol. Monogr. **4:** 351–389.

Denny, M. W. 1988. Biology and the mechanics of the wave-swept environment. Princeton Univ. Press.

———. 1995. Predicting physical disturbance: Mechanistic approaches to the study of survivorship on wave-swept shores. Ecol. Monogr. **65:** 371–418.

———, B. Helmuth, G. H. Leonard, C. D. G. Harley, L. J. Hunt, and E. K. Nelson. 2004. Quantifying scale in ecology: Lessons from a wave-swept shore. Ecol. Monogr. **74:** 513–532.

———, L. Miller, M. Stokes, L. Hunt, and B. Helmuth. 2003. Extreme water velocities: Topographical amplification of wave-induced flow in the surf zone of rocky shores. Limnol. Oceanogr. **48:** 1–8.

Emson, R. H., and R. J. Faller-Fritsch. 1976. An experimental investigation into the effect of crevice availability on abundance and size-structure in a population of *Littorina rudis* (Maton): Gastropoda: Prosobranchia. J. Exp. Mar. Biol. Ecol. **23:** 285–297.

Evans, R. G. 1947. The intertidal ecology of selected localities in the Plymouth neighborhood. J. Mar. Biol. Assoc. U.K. **27:** 173–218.

Gaines, S. D., and M. D. Bertness. 1993. The dynamics of juvenile dispersal: Why field ecologists must integrate. Ecology **74:** 2430–2435.

Gaylord, B. 1999. Detailing agents of physical disturbance: Wave-induced velocities and accelerations on a rocky shore. J. Exp. Mar. Biol. Ecol. **239:** 85–124.

———. 2000. Biological implications of surf-zone flow complexity. Limnol. Oceanogr. **45:** 174–188.

Helmuth, B. 1998. Intertidal mussel microclimates: Predicting the body temperature of a sessile invertebrate. Ecol. Monogr. **68:** 51–74.

———, and M. W. Denny. 2003. Predicting wave exposure in the rocky intertidal zone: Do bigger waves always lead to larger forces? Limnol. Oceanogr. **48:** 1338–1345.

———, and G. E. Hofmann. 2001. Microhabitats, thermal heterogeneity, and patterns of physiological stress in the rocky intertidal zone. Biol. Bull. (Woods Hole) **201:** 374–384.

Jones, K. M. M., and E. G. Boulding. 1999. State-dependent habitat selection by an intertidal snail: the costs of selecting a physically stressful microhabitat. J. Exp. Mar. Biol. Ecol. **242:** 149–177.

Jones, W. E., and A. Demetropoulos. 1968. Exposure to wave action: Measurements of an important ecological parameter on rocky shores on Anglesey. J. Exp. Mar. Biol. Ecol. **2:** 46–63.

Kinsman, B. 1965. Wind waves. Prentice Hall.

Koehl, M. A. R. 1984. How do benthic organisms withstand moving water? Amer. Zool. **24:** 57–70.

Lohse, D. P. 1993. The importance of secondary substratum in a rocky intertidal community. J. Exp. Mar. Biol. Ecol. **166:** 1–17.

Marchetti, K. E., and J. B. Geller. 1987. The effects of aggregation and microhabitat on desiccation and body temperature of the black turban snail, *Tegula funebralis* (A. Adams, 1855). Veliger **30:** 127–133.

McGuinness, K. A., and A. J. Underwood. 1986. Habitat structure and the nature of communities on intertidal boulders. J. Exp. Mar. Biol. Ecol. **104:** 97–123.

Menge, B. A. 1976. Organization of the New England rocky intertidal community: Role of predation, competition, and environmental heterogeneity. Ecol. Monogr. **46:** 355–393.

———. 1978. Predation intensity in a rocky intertidal community. Oecologia **34:** 1–16.

Paine, R. T., and S. A. Levin. 1981. Intertidal landscapes: Disturbance and the dynamics of pattern. Ecol. Monogr. **51:** 145–178.

Raffaelli, D. G., and R. N. Hughes. 1978. The effects of crevice size and availability on populations of *Littorina rudis* and *Littorina neritoides*. J. Anim. Ecol. **47:** 71–84.

Ricketts, E. F., and J. Calvin. 1939. Between Pacific tides, 5th ed. Stanford Univ. Press.

Rilov, G., Y. Benayahu, and A. Gasith. 2004. Life on the edge: Do biomechanical and behavioral adaptations to wave-exposure correlate with habitat partitioning in predatory whelks? Mar. Ecol. Prog. Ser. **282:** 193–204.

Shanks, A. L., and W. G. Wright. 1986. Adding teeth to wave action: The destructive effects of wave-borne rocks on intertidal organisms. Oecologia **69:** 420–428.

Somero, G. N. 2002. Thermal physiology and vertical zonation of intertidal animals: Optima, limits, and costs of living. Integr. Comp. Biol. **42:** 780–789.

Sousa, W. P. 1979. Experimental investigations of disturbance and ecological succession in a rocky intertidal algal community. Ecol. Monogr. **49:** 227–254.

Stephenson, T. A., and A. Stephenson. 1972. Life Between Tide Marks on Rocky Shores. Freeman.

Trussell, G. C. 1997*a*. Phenotypic plasticity in the foot size of an intertidal snail. Ecology **78:** 1033–1048.

———. 1997*b*. Phenotypic selection in an intertidal snail: Effects of a catastrophic storm. Mar. Ecol. Prog. Ser. **151:** 73–79.

———, A. S. Johnson, S. G. Rudolph, and E. S. Gilfillan. 1993. Resistance to dislodgment: Habitat and size-specific differences in morphology and tenacity in an intertidal snail. Mar. Ecol. Prog. Ser. **100:** 135–144.

Underwood, A. J. 2000. Experimental ecology of rocky intertidal habitats: What are we learning? J. Exp. Mar. Biol. Ecol. **250:** 51–76.

———. 2004. Landing on one's foot: Small-scale topographic features of habitat and the dispersion of juvenile intertidal gastropods. Mar. Ecol. Prog. Ser. **268:** 173–182.

———, and M. G. Chapman. 1989. Experimental analyses of the influences of topography of the substratum on movements and density of an intertidal snail, *Littorina unifasciata*. J. Exp. Mar. Biol. Ecol. **134:** 175–196.

———. 1996. Scales of spatial patterns of distribution of intertidal invertebrates. Oecologia **107:** 212–224.

———, and K. E. McFadyen. 1983. Ecology of the intertidal snail *Littorina acutispira*. J. Exp. Mar. Biol. Ecol. **66:** 169–197.

Wethey, D. S. 1985. Catastrophe, extinction, and species diversity: A rocky intertidal example. Ecology **66:** 445–456.

Received 21 February 2007
Amended 22 October 2007
Accepted 3 November 2007